

Azimuthal asymmetry in electro-production of neutral pions in semi-inclusive DIS

A. V. Efremov^{a*}, K. Goeke^b, P. Schweitzer^b

^a *Joint Institute for Nuclear Research, Dubna, 141980 Russia*

^b *Institute for Theoretical Physics II, Ruhr University Bochum, Germany*

Abstract

Recently HERMES has observed an azimuthal asymmetry A_{UL} in electro-production of neutral pions in semi-inclusive deep-inelastic scattering of unpolarized positrons off longitudinally polarized protons. This asymmetry (like those observed in the production of charged pions) is well reproduced theoretically by using the non-perturbative calculation of the proton transversity distribution h_1^q in the effective chiral quark-soliton model combined with experimental DELPHI-data on the new T-odd Collins fragmentation function H_1^\perp . There are no free, adjustable parameters in the analysis. Using the z -dependence of the HERMES azimuthal asymmetry and the calculated transversity distributions the z -dependence of the Collins fragmentation function is obtained. The value obtained from HERMES data is consistent with the DELPHI result, even though these results refer to different scales.

1 Introduction

Recently a large azimuthal asymmetry has been observed by HERMES in the electro-production of neutral pions in semi inclusive deep-inelastic scattering (SIDIS) of unpolarized positrons off longitudinally polarized protons [1]. A similarly large azimuthal asymmetry in the production of π^+ has been observed before, while no such azimuthal asymmetry was found in the production of π^- [2]. Azimuthal asymmetries were also observed in SIDIS off transversely polarized protons at SMC [3]. These asymmetries contain information on the proton transversity distributions the $h_1^q(x)$ and on the Collins fragmentation function $H_1^{\perp a}(z_h)$ ¹. The transversity distribution function $h_1^q(x)$ describes the distribution of transversely polarized quarks of flavour a in the nucleon [4]. The T-odd fragmentation function $H_1^{\perp a}(z_h)$ describes the left-right asymmetry in fragmentation of transversely polarized quarks of flavour a into a hadron [5, 6, 7, 9, 10] (the so-called "Collins asymmetry"). Both $H_1^{\perp a}(z_h)$ and $h_1^q(x)$ are twist-2, chirally odd, and not known experimentally. Only in the last years experimental indications to the T-odd fragmentation function $H_1^{\perp a}(z_h)$ in e^+e^- -annihilation have appeared [11, 12], while the HERMES and SMC experiments [1, 2, 3] can be viewed as the very first experimental indications to $h_1^q(x)$.

*Partially supported by RFBR grant 00-02-16696 and INTAS grant 01-587.

¹ We use the notation of the ref. [5, 6, 7].

Here we will explain the azimuthal asymmetry in π^0 production [1] by using information on H_1^\perp from DELPHI [11, 12] and the predictions from the chiral quark-soliton model (χ QSM) for the transversity distribution $h_1^a(x)$ [13]. Our analysis is free of any adjustable parameters. In this way the azimuthal asymmetries for π^\pm [2, 3] have been explained in Ref. [14]. We recalculate it using a bit more exact experimental cuts.

In order to use information from DELPHI on H_1^\perp , we have to assume that $\langle H_1^\perp \rangle / \langle D_1 \rangle$, the ratio of the T-odd to the usual fragmentation function (averaged over z_h and over flavours), varies little with scale. We will investigate whether this assumption is justified. For that we will use the prediction of $h_1^a(x)$ from χ QSM to extract $H_1^\perp(z)$ from z -dependence of HERMES data. We will show that the results for $\langle H_1^\perp \rangle / \langle D_1 \rangle$ from HERMES [1, 2], SMC [3] and DELPHI [11, 12] are consistent with each other.

2 Ingredients for analysis: h_1 and H_1^\perp

Transversity distribution function h_1 . We will take the predictions of the chiral quark-soliton model (χ QSM) as input for $h_1^a(x)$ [13].

The χ QSM is a quantum field-theoretical relativistic model with explicit quark and antiquark degrees of freedom. This allows an unambiguous identification of quark as well as antiquark distributions in the nucleon. Due to its field-theoretical nature the quark and antiquark distribution functions obtained in this model satisfy all general QCD requirements: positivity, sum rules, inequalities, etc [15]. The model results for the unpolarized quark and antiquark distribution function $f_1^a(x)$ and for the helicity quark distribution function $g_1^a(x)$ agree within (10 - 20)% with phenomenological parameterizations. This encourages confidence in the model predictions for $h_1(x)$. In Fig. 1 the results of the model are shown at the average $Q^2 = 4 \text{ GeV}^2$ close to the HERMES experiment.

The application of the model results has yet another advantage. When using the model results for twist-2 parton distributions it is consequent to neglect systematically twist-3 distributions for the following reason. The χ QSM has been derived from the instanton model of the QCD vacuum, and in the latter nucleon matrix elements of twist-3 operators are suppressed with respect to the leading twist-2 [16]. In the case of the twist-3 distribution $\tilde{h}_L(x)$ this has been shown explicitly in Ref. [17].

The T-odd fragmentation function H_1^\perp . The Collins fragmentation function $H_1^\perp(z_h, \mathbf{k}_\perp^2)$ describes a left-right asymmetry in the fragmentation of a transversely polarized quark with spin $\boldsymbol{\sigma}$ and momentum $\mathbf{k} = (\mathbf{k}_L, \mathbf{k}_\perp)$ into a hadron with momentum $\mathbf{P}_h = z_h \mathbf{k}$: the relevant structure is $H_1^\perp(z_h, \mathbf{k}_\perp^2) \boldsymbol{\sigma}(\mathbf{k} \times \mathbf{P}_{\perp h}) / (|\mathbf{k}| \langle P_{\perp h} \rangle)$. Here $\langle P_{\perp h} \rangle$ is the average transverse momentum of the final hadron².

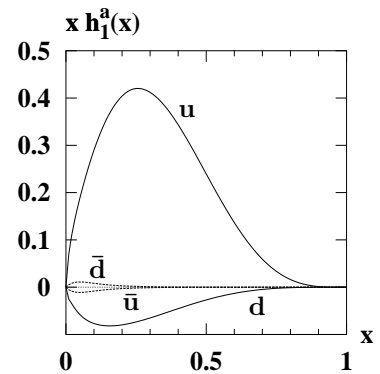


Figure 1: The chiral quark-soliton model prediction for the proton $xh_1^a(x)$ vs. x at the scale $Q^2 = 4 \text{ GeV}^2$. The u -quark dominates the proton transversity distribution.

² Notice the different normalization factor compared to [5, 6, 7], $\langle P_{h\perp} \rangle$ instead of M_h .

This fragmentation function is responsible for a specific azimuthal asymmetry of a hadron in a jet around the axis in direction of the second hadron in the opposite jet. This asymmetry was measured using the DELPHI data collection [11]. For the leading particles in each jet of two-jet events, averaged over quark flavors (assuming $H_1^\perp = \sum_h H_1^{\perp q/h}$ is flavor independent), the most reliable value of the analyzing power is given by

$$\left| \frac{\langle H_1^\perp \rangle}{\langle D_1 \rangle} \right| = (6.3 \pm 2.0)\% \quad (1)$$

with presumably large systematic errors³. The result Eq.(1) refers to the scale M_Z^2 and to an average over \mathbf{k}_\perp and over z_h with $\langle z_h \rangle \simeq 0.4$ [11].

3 The HERMES experiment for A_{UL}

In the HERMES experiment [1] the cross section for $lp \rightarrow l'\pi^0 X$ was measured in dependence of the azimuthal angle ϕ_h , which is the angle between lepton scattering plane and the plane defined by momentum \mathbf{q} of virtual photon and momentum \mathbf{P}_h of produced pion, see Fig. 2.

Denoting momentum of the target proton by P , momentum of the incoming lepton by l and momentum of the outgoing lepton by l' , the relevant kinematical variables – center of mass energy square s , four momentum transfer q , invariant mass of the photon-proton system W , x , y and z_h – are defined as

$$\begin{aligned} s &:= (P + l)^2, & q &:= l - l', & Q^2 &:= -q^2, \\ W^2 &:= (P + q)^2 = s(1 - x)y + M_N^2 \\ x &:= \frac{Q^2}{2Pq}, & y &:= \frac{2Pq}{s} & \text{and} & z_h := \frac{PP_h}{Pq}. \end{aligned} \quad (2)$$

In this notation the azimuthal asymmetry $A_{UL}^{\sin\phi_h}(x)$ measured by HERMES reads

$$A_{UL}^{\sin\phi_h}(x) = \frac{\int dy dz_h d\phi_h \sin\phi_h \left(\frac{1}{S^+} \frac{d^4\sigma^+}{dx dy dz_h d\phi_h} - \frac{1}{S^-} \frac{d^4\sigma^-}{dx dy dz_h d\phi_h} \right)}{\frac{1}{2} \int dy dz_h d\phi_h \left(\frac{d^4\sigma^+}{dx dy dz_h d\phi_h} + \frac{d^4\sigma^-}{dx dy dz_h d\phi_h} \right)}. \quad (3)$$

The subscript “ U ” reminds of the unpolarized beam, and “ L ” reminds of the longitudinally (with respect to the beam direction) polarized proton target. S^\pm denotes the proton spin, where “+” means polarization opposite to the beam direction. When integrating over y and z_h one has to consider the experimental cuts

$$W^2 > W_{\min}^2 = 4 \text{ GeV}^2, \quad Q^2 > Q_{\min}^2 = 1 \text{ GeV}^2, \quad 0.2 < y < 0.85, \quad 0.2 < z_h < 0.7. \quad (4)$$

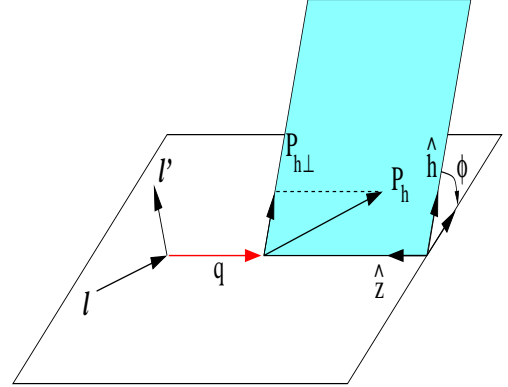


Figure 2: Kinematics of the process $lp \rightarrow l'\pi X$ in the lab frame. In the HERMES experiment the lepton l is a positron.

³ A similar value was also obtained from the pion asymmetry in inclusive pp -scattering [19].

The azimuthal asymmetry. The cross sections entering the asymmetry $A_{UL}^{\sin\phi_h}$ Eq. (3) have been computed in Ref. [8] at tree-level up to order $1/Q$. The denominator in Eq. (3) is the cross section for pion production from scattering of unpolarized positrons on unpolarized target protons

$$\frac{1}{2} \left(\frac{d^3\sigma^+}{dx dy d\phi_h} + \frac{d^3\sigma^-}{dx dy d\phi_h} \right) = \frac{d^3\sigma_{UU}}{dx dy d\phi_h} . \quad (5)$$

The numerator in Eq. (3) consists of two parts – a longitudinal and a transverse part with respect to the photon momentum \mathbf{q}

$$\frac{1}{S^+} \frac{d^3\sigma^+}{dx dy d\phi_h} - \frac{1}{S^-} \frac{d^3\sigma^-}{dx dy d\phi_h} = \frac{2}{S} \frac{d^3\sigma_{UL}}{dx dy d\phi_h} + \frac{2}{S} \frac{d^3\sigma_{UT}}{dx dy d\phi_h} . \quad (6)$$

The cross sections are given by

$$\begin{aligned} \frac{d^4\sigma_{UU}}{dx dy dz_h d\phi_h} &= \frac{\alpha^2 s}{Q^4} \left(1 + (1-y)^2 \right) \sum_a e_a^2 x f_1^a(x) D_1^a(z_h) \\ \frac{d^4\sigma_{UL}}{dx dy dz_h d\phi_h} &= \sin\phi_h S_L \frac{\alpha^2 s}{Q^4} \frac{M_N}{Q} \frac{8(2-y)\sqrt{1-y}}{\langle z_h \rangle \sqrt{1 + \langle \mathbf{P}_{\perp N}^2 \rangle / \langle \mathbf{k}_{\perp}^2 \rangle}} \sum_a e_a^2 x^3 \int_x^1 \frac{d\xi}{\xi^2} h_1^a(\xi) H_1^{\perp a}(z_h) \\ \frac{d^4\sigma_{UT}}{dx dy dz_h d\phi_h} &= \sin\phi_h S_T \frac{\alpha^2 s}{Q^4} \frac{2(1-y)}{\langle z_h \rangle \sqrt{1 + \langle \mathbf{P}_{\perp N}^2 \rangle / \langle \mathbf{k}_{\perp}^2 \rangle}} \sum_a e_a^2 x h_1^a(x) H_1^{\perp a}(z_h) . \end{aligned} \quad (7)$$

In Eq. (7) terms have been omitted which vanish after the (weighted) integration over ϕ_h , and pure twist-3 contributions have been systematically neglected for reasons mentioned above so that for h_L entering σ_{UL} the Wandzura-Wilczek type relation $h_L(x) = 2x \int_x^1 d\xi \frac{h_1(\xi)}{\xi^2}$ is hold (see Ref. [8] and Appendix). A term proportional to $\tilde{H}_1^\perp(z_h)$ is also neglected, even though it contains a twist two contribution due to $\tilde{H}_1^\perp(z_h) = z_h \frac{d}{dz_h} H_1^\perp(z_h) + \text{twist-3}$. However the contribution of this term to σ_{UL} is very small, see the Appendix. $\langle \mathbf{P}_{\perp N}^2 \rangle$ and $\langle \mathbf{k}_{\perp}^2 \rangle = \langle \mathbf{P}_{\perp h}^2 \rangle / \langle z_h^2 \rangle$ are the mean square transverse momenta of quarks in the distribution and fragmentation functions, respectively. S_L is the longitudinal, S_T is the transverse component of target spin S with respect to the 3-momentum of the virtual photon

$$S_L = S \cos\theta_\gamma \simeq S \left(1 - \frac{2M_N^2 x(1-y)}{sy} \right) , \quad S_T = S \sin\theta_\gamma \simeq S \sqrt{\frac{4M_N^2 x(1-y)}{sy}} , \quad (8)$$

where θ_γ is the angle of virtual photon with respect to incoming beam. Assuming isospin symmetry and favored fragmentation the following relations hold

$$\begin{aligned} D_1^{u/\pi^+} = D_1^{\bar{d}/\pi^+} = D_1^{d/\pi^-} = D_1^{\bar{u}/\pi^-} &\gg D_1^{d/\pi^+} = D_1^{\bar{u}/\pi^+} = D_1^{u/\pi^-} = D_1^{\bar{d}/\pi^-} \simeq 0 \\ D_1^{u/\pi^0} = D_1^{\bar{u}/\pi^0} = D_1^{d/\pi^0} = D_1^{\bar{d}/\pi^0} &\text{ and } D_1^{u/\pi^+} = D_1^{d/\pi^-} = \frac{1}{2} D_1^{u/\pi^0} \stackrel{\text{def.}}{=} D_1 , \end{aligned} \quad (9)$$

where the arguments z_h are omitted. The same relations hold for H_1^\perp . Inserting Eq. (7) and (9) into Eq. (3) for the azimuthal asymmetry $A_{UL}^{\sin\phi_h}$ yields for the production of the

pion π

$$A_{UL}^{\sin\phi}(x, \pi) = \frac{1}{\langle z_h \rangle \sqrt{1 + \langle \mathbf{P}_{\perp N}^2 \rangle / \langle \mathbf{k}_{\perp}^2 \rangle}} \frac{\langle H_1^\perp \rangle}{\langle D_1 \rangle} \times \left(B_L(x) \frac{\sum_a^\pi e_a^2 x^2 \int_x^1 d\xi h_1^a(\xi) / \xi^2}{\sum_{a'}^\pi e_{a'}^2 f_1^{a'}(x)} + B_T(x) \frac{\sum_a^\pi e_a^2 h_1^a(x)}{\sum_{a'}^\pi e_{a'}^2 f_1^{a'}(x)} \right), \quad (10)$$

where \sum_a^π means summation only over those flavours which contribute to the favoured fragmentation into the specific pion asymmetry, i.e. in the π^0 case e.g.

$$\frac{\sum_a^{\pi^0} e_a^2 h_1^a(x)}{\sum_{a'}^{\pi^0} e_{a'}^2 f_1^{a'}(x)} = \frac{(4h_1^u + 4h_1^{\bar{u}} + h_1^d + h_1^{\bar{d}})(x)}{(4f_1^u + 4f_1^{\bar{u}} + f_1^d + f_1^{\bar{d}})(x)}.$$

The prefactors $B_L(x)$, $B_T(x)$ introduced in Eq. (10) are given by

$$B_L(x) = \frac{\int dy 8(2-y) \sqrt{1-y} \cos\theta_\gamma M_N / Q^5}{\int dy (1 + (1-y)^2) / Q^4} \quad \text{and} \quad B_T(x) = \frac{\int dy 2(1-y) \sin\theta_\gamma / Q^4}{\int dy (1 + (1-y)^2) / Q^4}. \quad (11)$$

When integrating over $y \in [y_1(x), y_2(x)]$ one has to keep in mind that Q , $\sin\theta_\gamma$ and $\cos\theta_\gamma$ are functions of x and y , according to Eq. (2) and Eq. (8). The x -dependent integration range of variable y is due to the experimental cuts Eq. (4)

$$y_1(x) := \max\left(0.2, \frac{Q_{\min}^2}{sx}, \frac{W_{\min}^2 - M_N^2}{s(1-x)}\right) \leq y \leq y_2(x) := 0.85. \quad (12)$$

The implicit dependence of h_1^a , f_1^a , $H_1^{\perp a}$ and D_1^a on y through Q is neglected. The distributions will be taken at the average value $Q_{\text{av}}^2 = 4 \text{ GeV}^2$ close to the HERMES experiment.

Results. In the HERMES experiment $\langle \mathbf{P}_{\perp N}^2 \rangle \simeq \langle \mathbf{P}_{\perp h}^2 \rangle = \langle z_h^2 \rangle \langle \mathbf{k}_{\perp}^2 \rangle$ and $\langle z_h \rangle = 0.41$. Approximating $\langle z_h^2 \rangle \simeq \langle z_h \rangle^2$ and using the result Eq. (1), the overall prefactor in Eq. (10) is

$$\frac{1}{\langle z_h \rangle \sqrt{1 + \langle \mathbf{P}_{\perp N}^2 \rangle / \langle \mathbf{k}_{\perp}^2 \rangle}} \frac{\langle H_1^\perp \rangle}{\langle D_1 \rangle} = 0.12 \pm 0.04. \quad (13)$$

The error is due to the experimental error of the analyzing power $\langle H_1^\perp \rangle / \langle D_1 \rangle$ Eq. (1), of which only the modulus is known. Here we have chosen the positive sign, for which the analysis of azimuthal asymmetries for π^\pm gave evidence for [14]. When using the DELPHI result Eq. (1) to explain the HERMES experiment, we assume a weak scale dependence of the analyzing power. For $h_1^a(x)$ we take the results of the chiral quark-soliton model [13] and for $f_1^a(x)$ the parameterization from Ref. [18], both LO-evolved to the average scale $Q_{\text{av}}^2 = 4 \text{ GeV}^2$. It is instructive to investigate how much the longitudinal spin (twist-3) part and the transverse spin (twist-2) part contribute to the total azimuthal asymmetry $A_{UL}^{\sin\phi}(x)$. Comparing the x -dependent prefactors $B_L(x)$ and $B_T(x)$ Eq. (11), we note that $B_L(x) \gg B_T(x)$, see Fig. 3a. This is due to the fact that $\cos\theta_\gamma \simeq 1$ appears in $B_L(x)$, while in $B_T(x)$ we have $\sin\theta_\gamma = \mathcal{O}(M_N/\sqrt{s})$ which is very small. However this effect is partially canceled by the fact that $x^2 \int_x^1 dy h_1^a(y) / y^2$, which contributes to the longitudinal (twist-3) part, is much smaller than $h_1^a(x)$, which contributes to the transverse (twist-2) part. The

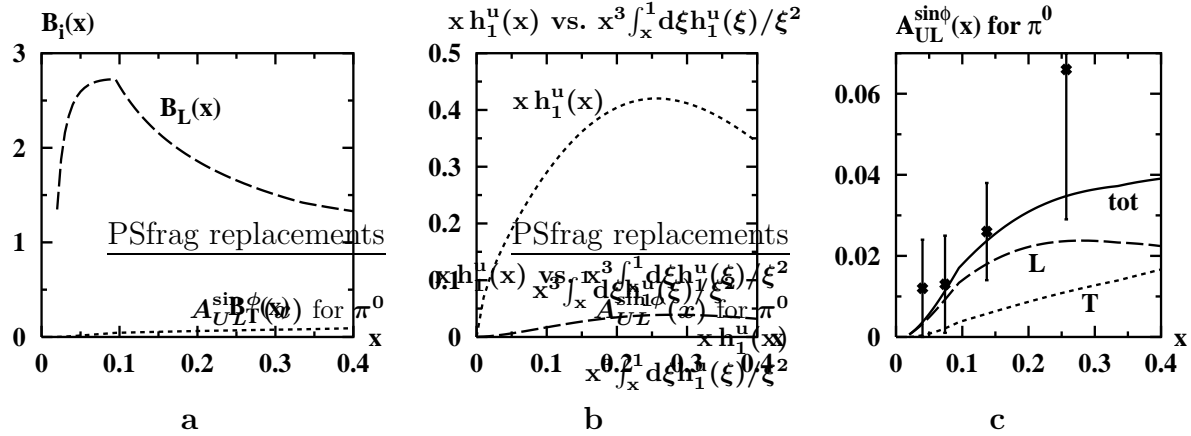


Figure 3: **a.** The prefactors $B_L(x)$ (dashed) and $B_T(x)$ (dotted line) – as defined in Eq. (11) – vs. x . Clearly $B_L(x) \gg B_T(x)$ for HERMES kinematics.

Figure 3: **b.** $x^3 \int_x^1 d\xi h_1^u(\xi)/\xi^2$ (dashed) and $xh_1^u(x)$ (dotted line) at $Q^2 = 4 \text{ GeV}^2$ vs. x . One observes that $xh_1^u(x) \gg x^3 \int_x^1 d\xi h_1^u(\xi)/\xi^2$. The situation is similar for other flavours.

Figure 3: **c.** The contribution of longitudinal (L, dashed) and transverse (T, dotted) spin part to the total (tot, solid line) azimuthal π^0 asymmetry $A_{UL}^{\sin\phi}(x)$ and data from [1] vs. x .

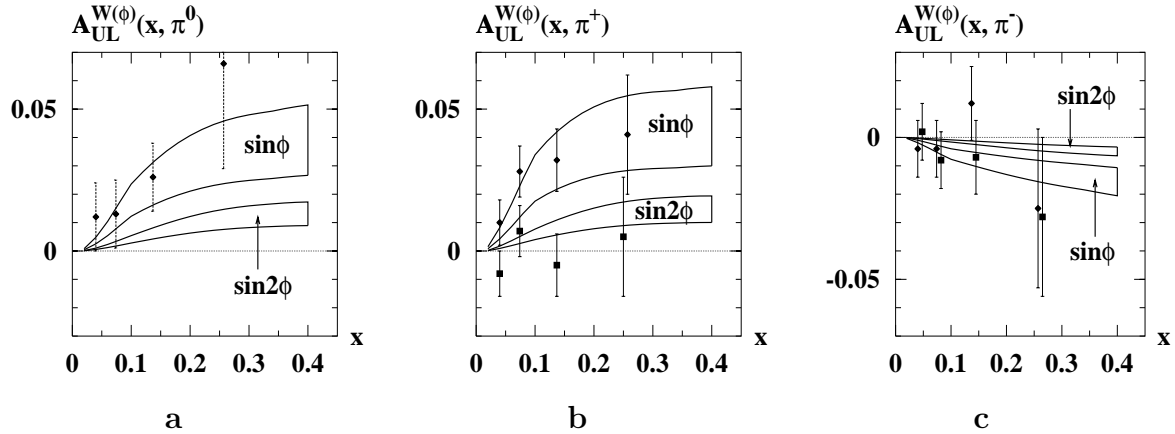


Figure 4: Azimuthal asymmetries $A_{UL}^{W(\phi)}(x, \pi)$ weighted by $W(\phi) = \sin\phi$ and $\sin 2\phi$, respectively, for π^0 (a), π^+ (b) and π^- (c) as function of x . The rhombs denote data on $A_{UL}^{W(\phi)}(x, \pi)$, the squares data on $A_{UL}^{\sin 2\phi}(x, \pi)$ from Ref. [1, 2]. The enclosed areas correspond to the azimuthal asymmetries evaluated using the prediction of the chiral quark-soliton model for $h_1^a(x)$ and the DELPHI result for the analyzing power $\langle H_1^\perp \rangle / \langle D_1 \rangle = (6.3 \pm 2.0)\%$ [11], and take into account the statistical error of the analyzing power.

results of the chiral quark-soliton model for $h_1^a(x)$ satisfy $x^2 \int_x^1 dy h_1^a(y)/y^2 < 0.1 h_1^a(x)$ in the whole x region. In Fig. 3b this is demonstrated for the u quark. As a result the longitudinal and the transverse part give – with increasing x – comparably large contributions to the total $A_{UL}^{\sin\phi}(x)$. However, the longitudinal part gives the major contribution in the whole x region, see Fig. 3c. The results shown in Fig. 3c correspond to the central value of the numerical prefactor, Eq. (13). For comparison data from Ref. [1] are included in Fig. 3c.

Repeating the same steps for charged pions, we obtain the results shown in Fig. 4. In this figure we compare the HERMES data on $A_{UL}^{\sin\phi_h}(x)$ (and for $A_{UL}^{\sin 2\phi_h}(x)$) for π^0 , π^+ and

Asymmetry	χ QSM [13] + DELPHI [11]	HERMES exp. [1, 2]
$A_{UL}^{\sin\phi}$		
π^0	0.017 ± 0.005	$0.019 \pm 0.007 \pm 0.003$
π^+	0.024 ± 0.008	$0.022 \pm 0.005 \pm 0.003$
π^-	-0.0046 ± 0.0015	$-0.002 \pm 0.006 \pm 0.004$
$A_{UL}^{\sin 2\phi}$		
π^0	0.0044 ± 0.0014	$0.006 \pm 0.007 \pm 0.003$
π^+	0.0063 ± 0.0020	$-0.002 \pm 0.005 \pm 0.010$
π^-	-0.0011 ± 0.0003	$-0.005 \pm 0.006 \pm 0.005$

Table 1: The integrated azimuthal asymmetries $A_{UL}^{\sin\phi}$ and $A_{UL}^{\sin 2\phi}$ for π^+ , π^0 and π^- . 2nd column: Results obtained with the chiral quark-soliton model prediction for proton transversity distribution $h_1^a(x)$ [13] and the DELPHI result for H_1^\perp [11]. The error is due to the statistical error of the DELPHI result, Eq. (1). 3rd column: Experimental data from HERMES [1, 2].

π^- [1, 2] with the results which follow from our analysis. The results shown here differ slightly from those obtained previously in Ref. [14] since there the lower y -cut was taken to be $y > 0$, instead of $y > 0.2$, see Eq. (4).

Finally, integrating the azimuthal asymmetries (numerator and denominator separately) over the x -region covered by the HERMES experiment, $0.023 \leq x \leq 0.4$, we obtain the results for $A_{UL}^{\sin\phi_h}$ and $A_{UL}^{\sin 2\phi_h}$ for π^0 and π^\pm production which are summarized in Table 1. We conclude that the azimuthal asymmetries obtained with the chiral quark-soliton model prediction for $h_1^a(x)$ [13] combined with the DELPHI result for the analyzing power [11] are consistent with experiment.

4 Determining $H_1^\perp(z_h)$

We used the DELPHI result for the analyzing power $\langle H_1^\perp \rangle / \langle D_1 \rangle$, Eq. (1), in order to explain the HERMES experiment. When doing so we presumed that the analyzing power varies weakly with scale. This assumption can be questioned. Therefore let us reverse the logic here, and use the HERMES results for the π^0 and π^+ azimuthal asymmetries to estimate $H_1^\perp(z_h)/D_1(z_h)$. For that we will use the chiral-quark soliton model prediction for $h_1^a(x)$, and this will introduce a model dependence. However, since the results of the model for known distribution functions agree within (10 – 20)% with parameterizations, we expect a similar “accuracy” for the model prediction for $h_1(x)$. With this in mind, the model dependence can be viewed as an additional systematic error, which however is “under control” and of order (10 - 20)%.

From the HERMES data on $A_{UL}^{\sin\phi_h}(z)$ for π^0 and π^+ we obtain the results shown in Fig.

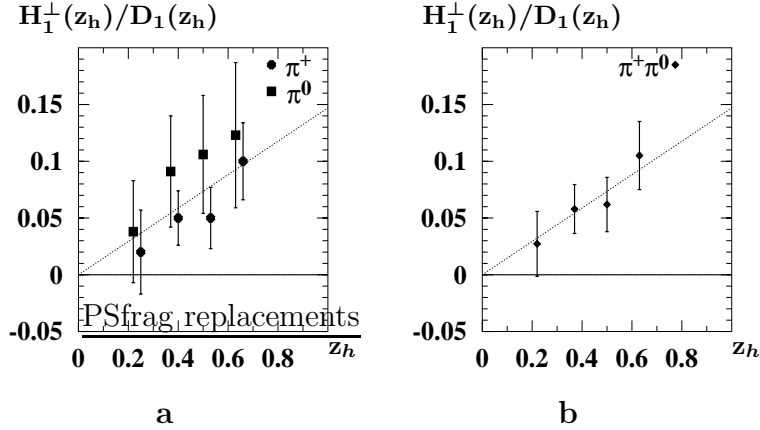


Figure 5: **a.** $H_1^\perp(z_h)/D_1^\perp(z_h)$ vs. z_h , as extracted from HERMES data [1, 2] on the azimuthal asymmetries $A_{UL}^{\sin\phi}(z_h)$ for π^+ and π^0 production using the prediction of the chiral quark-soliton model for $h_1^a(x)$ [13]. The error-bars are due to the statistical error of the data.

Figure 5: **b.** The same as Fig. 5a with data points from π^+ and π^0 combined. The line plotted in both figures is the best fit to the form $H_1^\perp(z_h)/D_1^\perp(z_h) = a z_h$ with $a = 0.15$.

5. The data can be described by the fit $H_1^\perp(z_h)/D_1(z_h) = a z_h$ with

$$H_1^\perp(z_h) = a z_h D_1(z_h) \quad \text{with} \quad a = \text{const} = 0.15 \pm 0.03 . \quad (14)$$

The error is the statistical error of the HERMES data. One should keep in mind that there is also a systematical error of the HERMES data (which varies with z_h), and a systematical error due to the uncertainty of the theoretical calculation of $h_1^a(x)$.

Averaging over z_h we obtain

$$\frac{\langle H_1^\perp \rangle}{\langle D_1 \rangle} = \begin{cases} (5.8 \pm 1.3 \pm 0.8)\% & \text{from HERMES } \pi^+ \text{ data} \\ (7.1 \pm 2.6 \pm 0.8)\% & \text{from HERMES } \pi^0 \text{ data} \\ (6.1 \pm 0.9 \pm 0.8)\% & \text{combined HERMES result.} \end{cases} \quad (15)$$

Here the statistical and the systematical errors of the HERMES data are considered. Again one should keep in mind an additional error of (10 - 20)% due to the uncertainty of theoretical prediction for $h_1^a(x)$.

Note that from the SMC data for the azimuthal asymmetry in the production of charged hadrons in SIDIS off transversely polarized protons [3], we obtain in this way the value

$$\frac{\langle H_1^\perp \rangle}{\langle D_1 \rangle} = (10 \pm 5)\% \quad \text{from SMC data.} \quad (16)$$

The results for the analyzing power from HERMES Eq. (15), SMC Eq. (16) and DELPHI Eq. (1) are all consistent with each other. This indicates that the scale dependence of $\langle H_1^\perp \rangle / \langle D_1 \rangle$ might be indeed weak.

The observation that $H_1^\perp(z_h) \propto z_h D_1(z_h)$ – if it will be confirmed by future and more accurate data – is physically very appealing. The smaller the momentum fraction transferred from the parent parton to the hadron, the less the produced hadron knows about the polarization of the parton.

We would like to thank M. V. Polyakov and K. A. Oganessyan and O. Teryaev for fruitful discussions, B. Dressler for providing the evolution code, and D. Hasch from the HERMES collaboration for clarifying questions on experimental cuts. A.E. is thankful to the Institute of Theoretical Physics II of Ruhr University Bochum for warm hospitality.

A Azimuthal asymmetries

Unpolarized cross section σ_{UU} . The unpolarized differential cross section follows from Eq. (113) of Ref. [8]

$$\frac{d^5\sigma_{UU}}{dx dy dz_h d^2\mathbf{P}_{\perp h}} = \frac{4\pi\alpha^2 s}{Q^4} \sum_{a,\bar{a}} e_a^2 \left\{ \frac{1 + (1-y)^2}{2} x f_1^a(x) D_1^a(z_h) + \dots \right\} \frac{\mathcal{G}(Q_{\perp}, R)}{z_h^2}. \quad (17)$$

The dots denote terms which cancel out after the integration over ϕ_h . $Q_{\perp} = |\mathbf{q}_{\perp}|$ and $\mathbf{q}_{\perp} = -(\mathbf{P}_{\perp h}/z_h)$. The dependence of the distribution and fragmentation functions on transverse quark momenta is assumed to be

$$\mathcal{G}(Q_{\perp}, R) = \frac{R^2}{\pi} \exp(-Q_{\perp}^2 R^2) \quad \text{with} \quad \int d^2\mathbf{P}_{\perp h} \frac{\mathcal{G}(Q_{\perp}, R)}{z_h^2} = 1. \quad (18)$$

After the integration over transverse momenta $d|\mathbf{P}_{\perp h}| |\mathbf{P}_{\perp h}|$, we obtain the spin averaged cross section Eq. (7)

$$\frac{d^3\sigma_{UU}}{dx dy d\phi_h} = \frac{\alpha^2 s}{Q^4} (1 + (1-y)^2) \sum_{a,\bar{a}} e_a^2 x f_1^a(x) \langle D_1^a(z_h) \rangle.$$

Longitudinal part σ_{UL} . The part of σ_{UL} which is proportional to $\sin\phi_h$ is given by Eq. (115) of Ref. [8]

$$\begin{aligned} \frac{d^5\sigma_{UL}^{\sin\phi_h}}{dx dy dz_h d^2\mathbf{P}_{\perp h}} &= \sin(\phi_h) S_L \frac{4\pi\alpha^2 s}{Q^4} 2(2-y)\sqrt{1-y} \frac{Q_{\perp}}{Q} \sum_a e_a^2 \\ &\times \left\{ \frac{R^6}{M_N \langle P_{\perp h} \rangle R_N^4 R_h^4} \left[\frac{R_h^2 - R_N^2}{R^2} - Q_{\perp}^2 R_h^2 \right] x h_{1L}^{\perp a}(x) H_1^{\perp a}(z_h) \right. \\ &+ \frac{M_N R^2}{\langle P_{\perp h} \rangle R_h^2} x^2 \tilde{h}_L^a(x) H_1^{\perp a}(z_h) \\ &\left. - \frac{M_h^2 R^2}{M_N \langle P_{\perp h} \rangle R_N^2} x h_{1L}^{\perp a}(x) \frac{\tilde{H}^a(z_h)}{z_h} \right\} \frac{\mathcal{G}(Q_{\perp}; R)}{z_h^2}. \quad (19) \end{aligned}$$

Here $R^2 = R_N^2 R_h^2 / (R_N^2 + R_h^2)$. Note the different normalization

$$\left. \frac{H_1^{\perp}}{M_h} \right|_{\text{Ref. [8]}} = \left. \frac{H_1^{\perp}}{\langle P_{\perp h} \rangle} \right|_{\text{here, Ref. [14]}}. \quad (20)$$

Let us decompose $\sigma_{UL}^{\sin\phi_h} = \sigma_{UL}^{\sin\phi_h}[H_1^{\perp}] + \sigma_{UL}^{\sin\phi_h}[\tilde{H}]$ and compute first the part $\sigma_{UL}^{\sin\phi_h}[H_1^{\perp}] \propto H_1^{\perp}$ in Eq. (19). Using the Wandzura–Wilczek type relation, Eq. (C11) in Ref. [8]

$$h_L(x, \mathbf{P}_{\perp N}^2) = -\frac{\mathbf{P}_{\perp N}^2}{M_N^2} \frac{h_{1L}^{\perp}(x, \mathbf{P}_{\perp N}^2)}{x} + \tilde{h}_L(x, \mathbf{P}_{\perp N}^2) + \mathcal{O}(m_q/M_N),$$

and neglecting quark mass terms, we arrive at the relation

$$\mathbf{P}_{\perp N}^2 h_{1L}^\perp(x, \mathbf{P}_{\perp N}^2) = M_N^2 x \left(\tilde{h}_L(x, \mathbf{P}_{\perp N}^2) - h_L(x, \mathbf{P}_{\perp N}^2) \right). \quad (21)$$

We have to reconsider the integration over the transverse quark momenta in the target nucleon. According to Eq. (D7) in Ref. [8] the term containing $h_{1L}^{\perp a}(x)$ in Eq. (19) arises from the convolution

$$I \left[(\hat{\mathbf{h}}\mathbf{P}_{\perp N}) (\mathbf{P}_{\perp N})^2 h_{1L}^\perp H_1^\perp \right] = \frac{Q_T R^6}{R_N^4 R_h^4} \left[\frac{R_h^2 - R_N^2}{R^2} - Q_\perp^2 R_h^2 \right] I[h_{1L}^\perp H_1^\perp] \\ \text{where } I[h_{1L}^\perp H_1^\perp] \equiv h_{1L}^{\perp a}(x) H_1^{\perp a}(z_h) \frac{\mathcal{G}(Q_\perp; R)}{z_h^2}. \quad (22)$$

If we insert the relation Eq. (21) into the above convolution Eq. (22) we obtain

$$I \left[(\hat{\mathbf{h}}\mathbf{P}_{\perp N}) (\mathbf{P}_{\perp N})^2 h_{1L}^\perp H_1^\perp \right] = \frac{M_N^2 Q_T R^2}{R_h^2} x \left(h_L(x) - \tilde{h}_L(x) \right) H_1^{\perp a}(z_h) \frac{\mathcal{G}(Q_\perp; R)}{z_h^2}, \quad (23)$$

due to Eq. (D5) in Ref. [8]. The result Eq. (23) we insert into the cross section Eq. (19) and observe that the contribution of $\tilde{h}_L^a(x)$ cancels out exactly

$$\frac{d^5 \sigma_{UL}^{\sin \phi_h} [H_1^\perp]}{dx dy dz_h d^2 \mathbf{P}_{\perp h}} = \sin(\phi_h) \frac{4\pi \alpha^2 s S_L}{Q^4} 2(2-y) \sqrt{1-y} \sum_a e_a^2 x^2 h_L^a(x) H_1^{\perp a}(z_h) \\ \times \frac{Q_\perp}{Q} \frac{M_N R^2}{\langle P_{\perp h} \rangle R_h^2} \frac{\mathcal{G}(Q_\perp; R)}{z_h^2}. \quad (24)$$

By means of Eq. (C19) in Ref. [8] we relate $h_L(x)$ to $h_1(x)$ as follows

$$h_L(x) = 2x \int_x^1 d\xi \frac{h_1(\xi)}{\xi^2} + \mathcal{O}(\tilde{h}_L) + \mathcal{O}(m_q/M_N), \quad (25)$$

and neglect systematically current quark mass terms and the twist-3 contribution \tilde{h}_L .

In the next step we integrate Eq. (24) over $|\mathbf{P}_{\perp h}| d|\mathbf{P}_{\perp h}|$. This yields

$$\frac{d^4 \sigma_{UL}^{\sin \phi_h} [H_1^\perp]}{dx dy dz_h d\phi_h} = \sin(\phi_h) \frac{4\pi \alpha^2 s S_L}{Q^4} 2(2-y) \sqrt{1-y} I_1 \sum_a e_a^2 x^2 h_L^a(x) H_1^{\perp a}(z_h), \quad (26)$$

where

$$I_1 \equiv \int d|\mathbf{P}_{\perp h}| |\mathbf{P}_{\perp h}| \frac{Q_\perp}{Q} \frac{M_N R^2}{\langle P_{\perp h} \rangle R_h^2} \frac{\mathcal{G}(Q_\perp; R)}{z_h^2} = \frac{M_N}{2\pi Q \langle z_h \rangle} \frac{1}{\sqrt{1 + \langle \mathbf{P}_{\perp N}^2 \rangle / \langle \mathbf{P}_h^{\perp 2} / z_h^2 \rangle}}. \quad (27)$$

When performing the integral I_1 we made use of the definitions

$$\langle Q_\perp \rangle \equiv \int d^2 \mathbf{Q}_\perp |\mathbf{Q}_\perp| \mathcal{G}(Q_\perp; R_h) = \frac{\sqrt{\pi}}{2R_h}, \quad \langle \mathbf{Q}_\perp^2 \rangle = \int d^2 \mathbf{Q}_\perp \mathbf{Q}_\perp^2 \mathcal{G}(Q_\perp; R_h) = \frac{1}{R_h^2}, \quad (28)$$

and analog $\langle P_N^\perp \rangle$ and $\langle \mathbf{P}_N^{\perp 2} \rangle$. We finally arrive at

$$\frac{d^4 \sigma_{UL}^{\sin \phi_h} [H_1^\perp]}{dx dy dz_h d\phi_h} = \sin(\phi_h) S_L \frac{\alpha^2 s}{Q^4} \frac{M_N}{Q} \frac{8(2-y) \sqrt{1-y}}{\langle z_h \rangle \sqrt{1 + \langle \mathbf{P}_{\perp N}^2 \rangle / \langle \mathbf{P}_h^{\perp 2} / z_h^2 \rangle}} \sum_a e_a^2 x^3 \int_x^1 d\xi \frac{h_1(\xi)}{\xi^2} H_1^{\perp a}(z_h). \quad (29)$$

Next we turn to the contribution $\sigma_{UL}[\tilde{H}] \propto \tilde{H}$. Note that \tilde{H} is normalized analogously to Eq. (20). After integration over $|\mathbf{P}_{\perp h}| d|\mathbf{P}_{\perp h}|$ we obtain

$$\frac{d^4 \sigma_{UL}^{\sin \phi_h}[\tilde{H}]}{dx dy dz_h d\phi_h} = -\sin(\phi_h) S_L \frac{4\pi\alpha^2 s}{Q^4} 2(2-y)\sqrt{1-y} I_2 \sum_a e_a^2 x h_{1L}^{\perp a}(x) \frac{\tilde{H}^a(z_h)}{z_h} \frac{\mathcal{G}(Q_{\perp}; R)}{z_h^2}, \quad (30)$$

where

$$I_2 = \int d|\mathbf{P}_{\perp h}| |\mathbf{P}_{\perp h}| \frac{Q_{\perp} M_h^2 R^2}{Q M_N R_N^2 \langle P_{\perp h} \rangle} = \frac{M_h^2 \langle z_h \rangle \langle \mathbf{P}_{\perp N}^2 \rangle}{8 Q M_N \langle P_{\perp h} \rangle^2} \frac{1}{\sqrt{1 + \langle \mathbf{P}_{\perp N}^2 \rangle / \langle \mathbf{P}_{\perp h}^2 / z_h^2 \rangle}}. \quad (31)$$

From Ref. [8], Eq. (C.15) and (C.19), we obtain the relation

$$h_{1L}^{\perp a}(x) = -\frac{M_N^2}{\langle \mathbf{P}_{\perp N}^2 \rangle} x \left(2x \int_x^1 d\xi \frac{h_1^a(\xi)}{\xi^2} + \dots \right), \quad (32)$$

where the dots denote twist-3 terms and contributions proportional to current quark masses, which we neglect. We also use the relation

$$\frac{\tilde{H}^a(z_h)}{z_h} = \frac{d}{dz_h} \left(z_h H_1^{\perp a}(z_h) \right) + \dots, \quad (33)$$

where we neglect consistently a twist-3 contribution, and obtain finally

$$\begin{aligned} \frac{d^4 \sigma_{UL}^{\sin \phi_h}[\tilde{H}]}{dx dy dz_h d\phi_h} &= \sin(\phi_h) S_L \frac{4\pi\alpha^2 s}{Q^4} (2-y)\sqrt{1-y} \frac{M_N M_h^2 \langle z_h \rangle}{2Q \langle P_{\perp h} \rangle^2} \\ &\times \frac{1}{\sqrt{1 + \langle \mathbf{P}_{\perp N}^2 \rangle / \langle \mathbf{P}_{\perp h}^2 / z_h^2 \rangle}} \sum_a e_a^2 x^3 \int_x^1 d\xi \frac{h_1^a(\xi)}{\xi^2} \frac{d}{dz_h} \left(z_h H_1^{\perp a}(z_h) \right). \end{aligned} \quad (34)$$

Thus we have the relation

$$\frac{d^4 \sigma_{UL}^{\sin \phi_h}[\tilde{H}]}{dx dy dz_h d\phi_h} = \frac{d^4 \sigma_{UL}^{\sin \phi_h}[H_1^{\perp}]}{dx dy dz_h d\phi_h} \cdot \frac{\pi M_h^2 \langle z_h \rangle^2}{4 \langle P_{\perp h} \rangle^2} \frac{d}{dz_h} (z_h H_1^{\perp}(z_h)) \ll \frac{d^4 \sigma_{UL}^{\sin \phi_h}[H_1^{\perp}]}{dx dy dz_h d\phi_h}, \quad (35)$$

if we assume a “reasonable” z_h -behaviour of the function $H_1^{\perp}(z_h)$.

Transverse part σ_{UT} . According to Eq. (116) in Ref. [8] the only term which is non-zero after the ($\sin \phi_h$ -weighted) integration over ϕ_h reads

$$\frac{d^5 \sigma_{UT}^{\sin \phi_h}}{dx dy dz_h d^2 \mathbf{P}_{\perp h}} = -\sin(\phi_h + \phi_s) S_T \frac{4\pi\alpha^2 s}{Q^4} (1-y) \frac{Q_{\perp} R^2}{\langle P_{\perp h} \rangle R_h^2} \sum_a x h_1^a(x) H_1^{\perp a}(z_h) \frac{\mathcal{G}(Q_{\perp}; R)}{z_h^2}, \quad (36)$$

with $\phi_s = -\pi$ for a longitudinally polarized target in the HERMES experiment. After the integration over transverse momenta we obtain the result quoted in Eq. (7)

$$\frac{d^4 \sigma_{UT}^{\sin \phi_h}}{dx dy dz_h d\phi_h} = \sin \phi_h S_T \frac{\alpha^2 s}{Q^4} \frac{2(1-y)}{\langle z_h \rangle \sqrt{1 + \langle z_h^2 \rangle \langle \mathbf{P}_{\perp N}^2 \rangle / \langle \mathbf{P}_{\perp h}^2 \rangle}} \sum_a x h_1^a(x) H_1^{\perp a}(z_h). \quad (37)$$

References

- [1] A. Airapetian *et al.*, hep-ex/0104005.
- [2] A. Airapetian *et al.*, Phys. Rev. Lett. **84** (2000) 4047, hep-ex/9910062.
H.Avakian, Nucl. Phys. (Proc. Suppl.) **B79** (1999) 523.
- [3] A.Bravar, Nucl. Phys. (Proc. Suppl.) **B79** (1999) 521.
- [4] J. Ralston and D. E. Soper, Nucl.Phys **B152** (1979) 109.
J. L. Cortes, B. Pire and J. P. Ralston, Z. Phys.**C55** (1992) 409.
R. L. Jaffe and X. Ji, Phys. Rev. Lett. **67** (1991) 552; Nucl. Phys **B375** (1992) 527.
- [5] D.Boer and P.J.Mulders, Phys. Rev. **D57** (1998) 5780.
- [6] D.Boer, R.Jakob and P.J.Mulders, Phys. Lett. **B424** (1998) 143.
- [7] P.J.Mulders and R.Tangerman, Nucl. Phys. **B461** (1995) 234.
D.Boer and R.Tangerman, Phys. Lett. **B381** (1996) 305.
- [8] P. J. Mulders and R. D. Tangerman, Nucl. Phys. B **461** (1996) 197,
[Erratum-ibid. B **484** (1996) 538], hep-ph/9510301.
- [9] J.Collins, Nucl. Phys. **B396** (1993) 161.
X.Artru and J.C.Collins, Z. Phys. **C69** (1996) 277.
- [10] A.Efremov, L.Mankiewicz and N.Törnqvist, Phys. Lett. **B284** (1992) 394.
- [11] A.V.Efremov, O.G.Smirnova and L.G.Tkatchev, Nucl. Phys. (Proc. Suppl.) **74** (1999) 49 and **79** (1999) 554; hep-ph/9812522.
- [12] A.V.Efremov *et al.*, Czech. J. Phys. **49** (1999) 75, Suppl. S2; hep-ph/9901216.
- [13] P. V. Pobylitsa and M. V. Polyakov, Phys. Lett. **B 389** (1996) 350.
P. Schweitzer, D. Urbano, M. V. Polyakov, C. Weiss, P. V. Pobylitsa, K. Goeke, Phys. Rev. D **64**, 034013 (2001), hep-ph/0101300.
- [14] A. V. Efremov, K. Goeke, M. V. Polyakov and D. Urbano, Phys. Lett. B **478** (2000) 94, hep-ph/0001119.
- [15] D.I. Diakonov, V.Yu. Petrov, P.V. Pobylitsa, M.V. Polyakov and C. Weiss, Nucl. Phys. **B 480** (1996) 341.
- [16] D. Diakonov, M. V. Polyakov and C. Weiss, hep-ph/9510232. Nucl. Phys. B **461** (1996) 539
- [17] B. Dressler and M. V. Polyakov, Phys. Rev. D **61** (2000) 097501, hep-ph/9912376.
- [18] M. Glück, E. Reya and A. Vogt, Z. Phys. **C 67** (1995) 433.
- [19] M. Boglione and P. J. Mulders, “Time-reversal odd fragmentation and distribution functions in pp and ep single spin asymmetries,” hep-ph/9903354.